Formation of deeply bound polar molecules combining pump-dump pulses with infrared radiation

Emanuel Fernandes de Lima [*]
Departamento de Física, Universidade Federal de São Carlos (UFSCar), São Carlos, São Paulo 13565-905, Brazil

(Received 26 September 2023; revised 11 December 2023; accepted 3 January 2024; published 18 January 2024)

We consider the formation of cold ground-state polar molecules in a low vibrational level by laser fields. Starting from a pair of cold colliding atoms of dissimilar species, we propose a strategy consisting of three steps. In the first step, a pump pulse induces the molecule formation by photoassociating the atomic pair in a high or intermediate vibrational level of an excited electronic molecular state. This step is followed by a dump pulse in an intermediate vibrational level of the ground state. The last step corresponds to the vibrational cooling or vibrational stabilization process. Taking advantage of the permanent dipole moment, an infrared chirped pulse induces downward transitions among the vibrational levels of the ground electronic state, reaching the ground vibrational level. We perform the strategy with with fixed-shaped pulses and also with an optimized chirped pulse for the stabilization step. To perform the optimization, we introduce an optimal control technique in which the optimization of the chirping is carried out in the time domain. This methodology has the benefit of limiting the pulse amplitude while focusing only on the frequency of the field. The proposed scheme is an alternative to the use of two pairs of pump-dump pulses or to the direct photoassociation and vibrational stabilization in the ground state.

DOI: 10.1103/PhysRevA.109.013315

I. INTRODUCTION

The formation of molecules from pairs of colliding atoms by the use of external fields is an important endeavor for Physics representing a very fundamental controlled chemical reaction [1–7]. Since direct cooling of molecules to ultracold temperatures is still challenging, assembling molecules from precooled atoms is a major means of creating ultracold molecules [8–13]. In particular, there is a special interest in forming ultracold gases of polar molecules due to their long-range dipole-dipole interaction [14–24]. Magnetoassociation followed by stimulated Raman adiabatic passage (STIRAP) provides a successful pathway for the formation of deeply bound molecules [25–29]. However, since magnetoassociation relies on the existence of favorable Feshbach resonances in the ground electronic state, alternative formation schemes must also be pursued.

Photoassociation reactions, in which the atoms are bound through the interaction of a laser field, constitute another main route leading to the formation of cold and ultracold molecules [30–39]. This process is commonly achieved by inducing a transition from the initial pair of atoms to an electronic excited molecular state using visible or ultraviolet radiation. To produce stable samples, the photoassociation process needs to be followed by a vibrational cooling or stabilization step, aiming at leaving the molecules in the vibrational ground level of the electronic ground state [40,41]. This second step can be performed by either spontaneous or induced emission [42,43]. A pair of pulses can be employed for this goal, the pump, photoassociating pulse, and the dump, stabilization pulse. However, to reach the ground vibrational level efficiently, two sequences of pump-dump pulses may be needed, possibly involving more than one excited electronic state [44,45].

In contrast with photoassociation processes which involve electronic excited states, it is, in principle, possible to perform both photoassociation and vibrational stabilization solely in the electronic ground state by means of far-infrared (IR) fields or terahertz radiation [46–50]. IR fields can induce free-bound and bound-bound transitions due to the existence of a nonnegligible permanent dipole moment of colliding atomic pair from distinct species. This approach, though restricted to heteronuclear molecules, has the benefit of not relying on the lifetime and structure of excited states. However, the coupling from the initial continuum levels representing the colliding atomic pair to the bound vibrational levels of the ground electronic are usually small compared to the coupling to bound vibrational levels of excited electronic states. Even if photoassociation is achieved within the ground state, the stabilization step through transitions among its vibrational levels may be hampered by the existence of forbidden or very week adjacent transitions at certain vibrational levels. This situation, which has been termed the *missing rung problem*, can be circumvented by inducing "multiple stepping" transitions to avoid such a missing rung [51–53].

The formation and vibrational stabilization of the molecules can be enhanced by the temporal shaping of the laser pulses involved in these processes. Optimal quantum control theory has been often invoked to accomplish this task with considerable success, but still with limited experimental implementations [54]. This can be attributed, in part, to the complexity of the optimized fields. A simpler and more feasible approach is the use of optimized linearly chirped pulses, for which the frequency varies linearly with time [55–58].

---

[*] eflima@ufscar.br

©2024 American Physical Society

Furthermore, with the increasing technological advances, considerable progress has been obtained with the use of shaped frequency chirps [59–63]. In a recent work, we proposed an analytical form of the time-dependent frequency of the laser pulse to perform photoassociation along with stabilization in the cold regime [51]. However, this approach only works for long pulse duration (tens of nanoseconds) and for low field amplitudes.

In the present work, we investigate the formation of cold heteronuclear molecules in deeply bound vibrational levels of the ground electronic state from cold colliding atoms. We propose a photoassociation and vibrational stabilization scheme based on three steps. The first two steps are carried out by a pair of pump-dump pulses, which induce the molecular formation in an excited electronic state and a subsequent transition to a intermediate vibrational level of the electronic ground state. The third step employs a chirped IR pulse to perform the final vibrational stabilization to the ground level. We start by implementing the proposed scheme with fixed-shape for the pump-dump pulses and linear chirped pulse for the vibrational stabilization step. Concerning the first photoassociation pulse, by optimizing the parameters of the its envelope, we verify that a rapidly turned on and slowly turned off pulse is very efficient to induce photoassociation as compared to symmetric turning on and off. This result is distinct from previous findings in which the photoassociation yields are enhanced by slowly turned on and rapidly turned off pulses [64,65]. We also apply quantum control theory to optimize the far-IR pulse where the optimization of the chirping is carried out in the time domain. This technique allows to accomplish the stabilization in a shorter time and with a lower amplitude than the linear chirp pulse. The numerical calculations are performed in a model system for the formation of LiCs molecules. Our scheme can be an alternative to the use of two pairs of pump-dump pulses and to the purely IR photoassociation in the ground state, exploring the strong coupling of the collision atomic pair with excited electronic state and also taking advantage of the existing permanent dipole moment for performing the stabilization with IR radiation, while avoiding the *missing rung problem*.

II. THREE-STEPS SCHEME FOR PHOTOASSOCIATION

We envisage a scenario of two cold atoms of different species colliding in the presence of an external laser field. The situation is described by means of two electronic states, the ground state and an electronic excited state, represented by the Hamiltonian

$$\hat{H}(t) = \hat{H}_0 - \varepsilon(t)\hat{\mu}, \tag{1}$$

with the molecular Hamiltonian $\hat{H}_0$ given by

$$\hat{H}_0 = \begin{pmatrix} \hat{T}_g + \hat{V}_g & 0 \\ 0 & \hat{T}_e + \hat{V}_e \end{pmatrix}, \tag{2}$$

where $\hat{T}$ denotes the kinetic energy operator, $\hat{V}$ the potential energy operator, while $\hat{\mu}$ is the dipole moment operator

$$\hat{\mu} = \begin{pmatrix} \hat{\mu}_g & \hat{\mu}_{ge} \\ \hat{\mu}_{ge} & \hat{\mu}_e \end{pmatrix}, \tag{3}$$

where the subscript g refers to the electronic ground state and the subscript e to the excited state. $\hat{\mu}_{ge}$ is the transition dipole moment between the ground and excited electronic states.

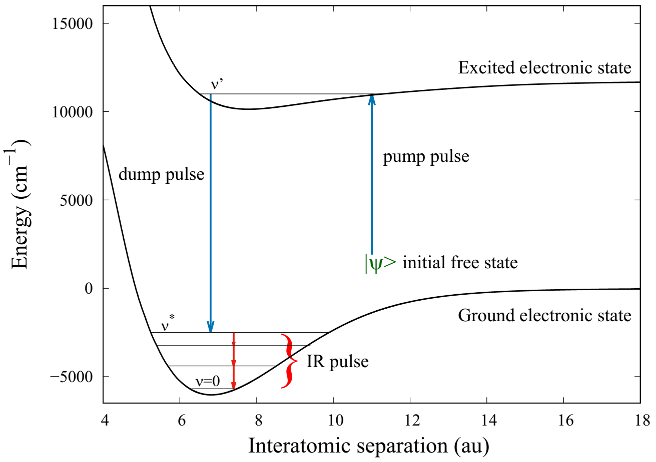

FIG. 1. Schematic diagram of the three-step photoassociation along with vibrational stabilization. In the first step, the pump pulse drives the initial unbound state to a vibrational level ν' of an excited electronic state. In the second step, the pump pulse drives a transition to an excited vibrational level ν^* of the electronic ground state. In the last step, an IR pulse performs further vibrational stabilization within the ground electronic state by driving downward transitions and reaching the vibration ground level $\nu = 0$.

The dynamics is given by the time-dependent Schrödinger equation

$$i\hbar\frac{\partial}{\partial t}|\psi(t)\rangle = \hat{H}|\psi(t)\rangle, \tag{4}$$

for the two-component wave function

$$\langle r|\psi(t)\rangle = \begin{pmatrix} \psi_g(r,t) \\ \psi_e(r,t) \end{pmatrix}, \tag{5}$$

where r is the interatomic distance. To capture the essential physics of the problem, we retain only the vibrational motion, neglecting the rotational motion, due to the low temperatures involved.

The external time-dependent electric field $\varepsilon(t)$ is composed of three pulses

$$\varepsilon(t) = \varepsilon_p(t) + \varepsilon_d(t) + \varepsilon_{\rm ir}(t), \tag{6}$$

where $\varepsilon_p(t)$ refers to the pump pulse, $\varepsilon_d(t)$ refers to the dump pulse, and $\varepsilon_{\rm ir}(t)$ refers to the infrared pulse. Figure 1 sketches the three-step scheme for forming polar molecules in their ground vibrational level. First, the initial unbound state $|\psi\rangle$, which represents the colliding atomic pair, is driven to a vibrational level ν' of an excited electronic state by a pump pulse. In the next step, the transition between ν' and an excited level ν^* of the ground electronic state is induced by a dump pulse. Finally, the last step consists of a vibrational stabilization step, where the transition from ν^* to the ground level $\nu = 0$ is induced by a single chirped IR pulse.

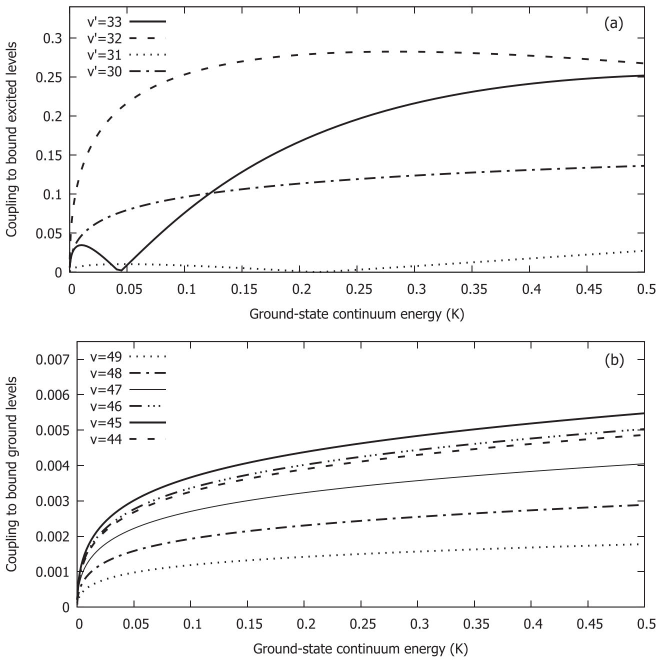

FIG. 2. (a) Dipole coupling between the free levels of the ground state and the bound levels of the excited state $|\langle\phi_{\nu'}|\hat{\mu}_{ge}|\phi_n\rangle|$. (b) Dipole coupling between the free levels of the ground state and its bound levels $|\langle\phi_\nu|\hat{\mu}_g|\phi_n\rangle|$.

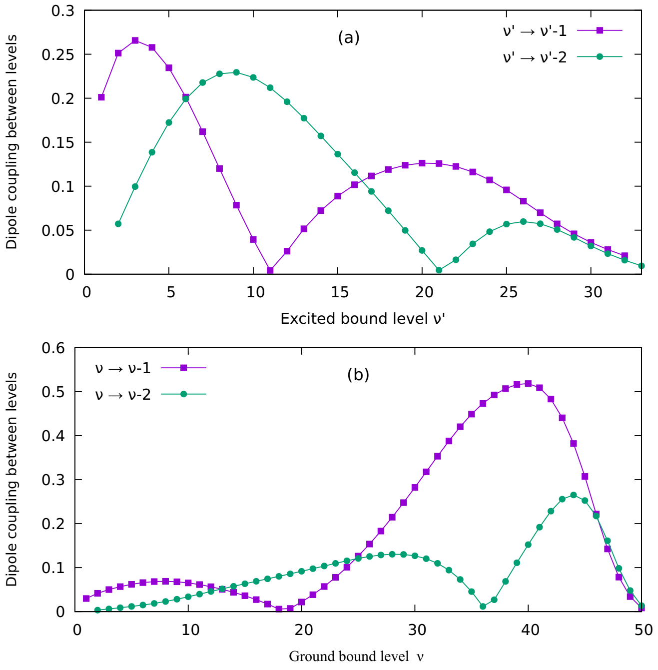

FIG. 3. (a) Dipole coupling between the bound levels of the excited state for $\Delta\nu' = -1$ and $\Delta\nu' = -2$ downward transitions $|\langle\phi_{\nu'}|\hat{\mu}_e|\phi_{\nu'+\Delta\nu'}\rangle|$. (b) Dipole coupling between the bound levels of the ground state for $\Delta\nu = -1$ and $\Delta\nu = -2$ transitions $|\langle\phi_\nu|\hat{\mu}_g|\phi_{\nu+\Delta\nu}\rangle|$.

III. MODEL FOR THE LiCs MOLECULE

The molecular potentials encompass discrete and continuum states. For a practical numerical solution, we discretize the continuum sectors by the introduction of a spatial grid [66]. The discrete energy levels of the ground state are labeled by E_ν with eigenfunctions $|\phi_\nu\rangle$, while the discretized continuum levels are labeled by E_n with eigenfunctions $|\phi_n\rangle$. The energies and eigenfunctions of the excited state are distinguished from the ground state by a prime symbol.

We illustrate the three-steps scheme considering the $X\,^1\Sigma$ and $B\,^1\Pi$ states of LiCs as the ground and excited potentials $V_g(r)$ and $V_e(r)$, respectively. The potential energy functions and dipoles' couplings were obtained from spline fittings based on data available in the literature [67–71]. The vibrational energies E_ν and eigenfunctions $|\phi_\nu\rangle$ of each electronic state were calculated by applying the B-splines technique with an exponential break-point sequence [72,73]. The calculations resulted in 51 vibrational bound levels for the ground state and 34 bound levels for the excited state. A large grid of size $r_{\max}$ was used to discretize the continuum ($r_{\max}$ of the order of 1500 atomic units).

Figure 2(a) shows the absolute value of the transition dipole moment $|\langle\phi_{\nu'}|\hat{\mu}_{ge}|\phi_n\rangle|$ from the continuum levels of the ground-electronic state to some top bound levels of the excited electronic state. The level $\nu' = 32$ possess the highest coupling in the entire range of continuum energies shown, revealing a possible starting point for the photoassociation process. We note that the lower vibrational levels of the excited state (not shown in the figure) have even smaller coupling. Figure 2(b) shows the dipole coupling between the continuum levels and the bound levels of the ground state $|\langle\phi_\nu|\hat{\mu}_g|\phi_n\rangle|$. An available route is for IR ground-state photoassociation is a transition to the $\nu = 45$ level, which has the highest coupling. However, these couplings are generally two orders of magnitude lower than the corresponding couplings to the excited bound levels.

Figure 3(a) shows the dipole couplings between bound levels of the excited state corresponding to $\Delta\nu' = -1$ and $\Delta\nu' = -2$ downward transitions $|\langle\phi_{\nu'}|\hat{\mu}_e|\phi_{\nu'+\Delta\nu'}\rangle|$. We note that vibrational stabilization within the excited state is possible, but there are some very small couplings for the one $\Delta\nu' = -1$ (at $\nu' = 11$) and $\Delta\nu' = -2$ transitions (at $\nu' = 21$), which should make the descending from the vibrational levels difficult. However, one can avoid these so-called "missing rungs" by switching from $\Delta\nu' = -1$ to $\Delta\nu' = -2$ transition frequencies [51,52]. We will not pursue the vibrational stabilization in the excited state since a more promising route is found in the ground electronic state. Figure 3(b) shows the downward transitions within the ground state. The gaps for the transitions (or missing rungs) are noted around $\nu = 19$ ($\Delta\nu = -1$) and $\nu = 36$ ($\Delta\nu = -2$). In contrast to the excited state, the couplings are larger between the top vibrational levels.

Figure 4 shows the absolute values of the transition dipole moments between some top levels of the excited state and the bound levels of the ground state $|\langle\phi_{\nu'}|\hat{\mu}_{ge}|\phi_\nu\rangle|$. It can be noted that these top levels have a very strong coupling with the very top levels of the ground state $\nu > 46$. However, as seen in Fig. 3(b), direct vibrational stabilization from such high levels would have to face the missing rungs. For clarity, the inset shows the couplings up to $\nu = 46$. It can be seen that the levels $\nu' = 31, 32, 33$ have considerable couplings to the

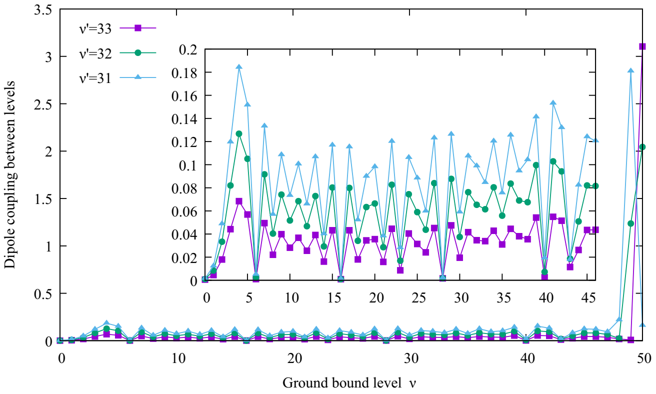

FIG. 4. Transition dipole moment from top levels of the electronic excited state to the bound levels of the ground state $|\langle\phi_{\nu'}|\hat{\mu}_{ge}|\phi_\nu\rangle|$. For clarity, the inset shows the couplings up to $\nu = 46$.

$\nu = 4$ level. Thus, once the excited level $\nu' = 32$ is populated, it can be transferred to the $\nu = 4$ state by the action of the dump pulse.

IV. FIXED-SHAPE PULSES

As seen in Fig. 2, for low temperatures, the coupling of the ground continuum with the excited bound levels are stronger than with the ground bound levels. The more favored route is to form a molecule in the $\nu' = 32$ level of the excited electronic state. This transition will be induced by the pump pulse. As noted in Fig. 4, there is a considerable coupling between the $\nu' = 32$ with the $\nu = 4$ of the ground state, which is induced by the dump pulse. Subsequently, the IR-chirped pulse drives the transition to the ground level. We note that this chosen pathway avoids the missing rungs both in the ground electronic state around the $\nu = 19$ level.

We consider the three-steps procedure with fixed shaped pulses

$$\varepsilon_i(t) = S_i(t) A_i \sin[\alpha_i(t)], \quad i = p, d, \mathrm{ir}, \tag{7}$$

where A_i is the peak amplitude of the ith pulse, while the envelope S_i is given by

$$S_i(t) = \begin{cases} \sin^2\left(\frac{\pi}{2}\frac{t-t_0^i}{t_u^i-t_0^i}\right), & \text{if } t_0^i < t < t_u^i, \\ 1, & \text{if } t_u^i < t < t_d^i, \\ \sin^2\left(\frac{\pi}{2}\frac{t+t_w^i-2t_d^i}{t_w^i-t_d^i}\right), & \text{if } t_d^i < t < t_w^i, \\ 0, & \text{otherwise,} \end{cases} \tag{8}$$

where $t_w^i - t_0^i$ defines the duration of the pulse that starts at $t = t_0^i$, while $t_u^i - t_0^i$ and $t_w^i - t_d^i$ set the times of smooth switching on and off, respectively.

The pump and dump pulses are chosen to be unchirped pulses, $\alpha_p = \omega_p t$ and $\alpha_d = \omega_d t$, while the IR pulse has a linear chirping rate

$$\alpha_{\mathrm{ir}} = \omega_{\mathrm{ir}} t + \tfrac{1}{2}\chi t^2. \tag{9}$$

We performed numerical calculations taking the initial wave function representing the atomic collision as a Gaussian wavepacket in the electronic ground state

$$\langle r|\psi(t=0)\rangle = \begin{pmatrix} \left(\frac{2}{\pi a^2}\right)^{1/4} \exp\left[\mathrm{i}\kappa r - \frac{(r-r_0)^2}{a^2}\right] \\ 0 \end{pmatrix}, \tag{10}$$

where a and r_0 define, respectively, the initial width and the central position of the wavepacket, while $\kappa < 0$ sets the initial collision momentum. For the time propagation, we considered an initial state with position $r_0 = 450$ a.u., width $a = 100$ a.u., and with collision energy corresponding to 50 mK. This wavepacket is placed far from the interaction region, i.e., at $t = 0$ the potentials and dipole functions are negligible over the wavepacket range. Although a description of a thermal gas of atoms would require a density operator representing a Boltzmann distribution [6], for s-wave collisions, the density operator can be decomposed to a set of Gaussian wavepackets [74]. An initial wavepacket is used often in the context of collision beam experiments [50]. In the present case, considering the initial Gaussian wavepacket facilitates the numerical calculations allowing us to demonstrate the proposed scheme.

As in previous works [46,75], we solve the time-dependent Schrödinger equation expanding the wave function in the basis of the energy eigenfunctions, and then truncating the number of discretized continuum levels for each electronic state. The expansion of Eq. (4) results in a coupled system of first-order differential equations for the coefficients. The unitary propagator $U(t, 0)$ is expressed in terms of a series of short time-step propagators $U(t + \Delta t, t)$ and each propagator is approximated by a second-order split operator, yielding the evolution of the wave function $|\psi(t + \Delta t)\rangle = U(t + \Delta t, t)|\psi(t)\rangle$. The number of discretized continuum levels considered was roughly 500 and 200 for the ground state and the excited state, respectively.

Figure 5 illustrates the three steps scheme with fixed-shape pulses. In Fig. 5(a), we show the dynamics of the relevant levels for the pump-dump pulses. The parameters of each pulse were optimized separately to yield the maximum population transfer. Thus, for the pump pulse, we optimized the parameters of the envelope t_u^p, t_d^p, t_0^p, t_w^p, and the amplitude A_p and the frequency ω_p. The same procedure was carried out for the dump pulse. We obtained for the pump pulse $\omega_p = 11\,731.47\,\mathrm{cm}^{-1}$, $A_p = 830\,\mathrm{V cm}^{-1}$, $t_0^p = 750$ ps, $t_w^p = 2500$ ps, $t_u^p = t_d^d = 810$ ps. We note that this is a rapidly turned on and slowly turned off pulse: it spends 60 ps from the start to attain the maximum amplitude, while it takes 2440 ps to switch-off the pulse. We obtain a population of roughly 0.89 in the $\nu' = 32$ level by the end of the pump pulse. The dump pulse is a π pulse, which transfers essentially all the population from the $\nu' = 32$ level to the $\nu = 4$ level with parameters $\omega_d = 16\,736.24\,\mathrm{cm}^{-1}$, $A_d = 4.4\,\mathrm{kV cm}^{-1}$, $t_0^d = 2850$ ps, $t_w^p = 700$ ps, $t_u^p = 2920$, $t_d^d = 3480$ ps.

Figure 5(b) illustrate the use of a linear chirp to perform the vibrational stabilization step starting with all population in the $\nu = 4$ state. In general, it can be obtained through high yields in the ground level, but at the cost of using fields with very high amplitudes. The results shown in the figure were obtained for a field amplitude of $V_{\mathrm{ir}} = 811\,\mathrm{kV cm}^{-1}$. The frequency ω_{ir} is chosen as the resonance frequency between the $\nu = 4$ and the $\nu = 3$ levels. The chirping rate is set as the difference between the resonance frequency of levels $\nu = 1$

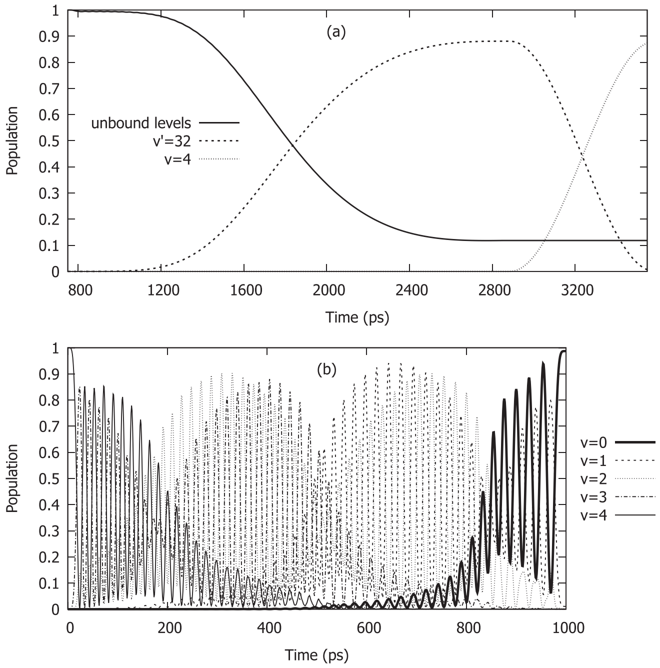

FIG. 5. Population dynamics of the relevant levels for the three-step scheme with fixed-shape pulses. (a) Dynamics for the pump-dump pulses. (b) Vibrational stabilization dynamics for a linear chirped pulse.

and $\nu = 0$, ω_{01}, and the frequency $\omega_{\rm ir}$, divided by the pulse duration $t_w^{\rm ir} = 1$ ns, i.e., $\chi = (\omega_{01} - \omega_{\rm ir})/t_w^{\rm ir}$. As we show in the next section, the optimization of the chirping can perform the stabilization process with considerably lower intensity.

V. OPTIMIZED CHIRPED PULSES

Consider the control problem of transferring some initial state $|\psi_0\rangle$ to a target vibrational level $|\phi_\nu\rangle$ in a time $t = t_f$ with a single pulse of the form of Eq. (7), where $\alpha(t)$ is the control function to be determined (for simplicity, we will drop here the index i). To this end, we define the extended functional J to be maximized,

$$J[\alpha] = |\langle\phi_\nu|\psi(t_f)\rangle|^2 - 2\mathrm{Re}\left\{\int_0^{t_f}\langle\chi(t)|\frac{\partial}{\partial t} + i\hat{H}[\alpha(t)]|\psi(t)\rangle\right\}, \tag{11}$$

where $|\psi(t)\rangle$ is the wave function driven by the pulse and $|\chi(t)\rangle$ is the Langrange multiplier introduced to assure satisfaction of the Schrödinger equation. The necessary condition for optimality $\delta J = 0$ yields the equations to be satisfied by the wave function, Lagrange multiplier, and optimal frequency

$$i\frac{\partial}{\partial t}|\psi(t)\rangle = \hat{H}[\alpha(t)]|\psi(t)\rangle, \tag{12}$$

with $|\psi(0)\rangle = |\psi_0\rangle$,

$$i\frac{\partial}{\partial t}|\chi(t)\rangle = \hat{H}[\alpha(t)]|\chi(t)\rangle, \tag{13}$$

with $|\chi(t_f)\rangle = |\phi_\nu\rangle\langle\phi_\nu|\psi(t_f)\rangle$ and

$$\mathrm{Im}\{\langle\chi(t)|\hat{\mu}|\psi(t)\rangle\}S(t)A\cos[\alpha(t)] = 0. \tag{14}$$

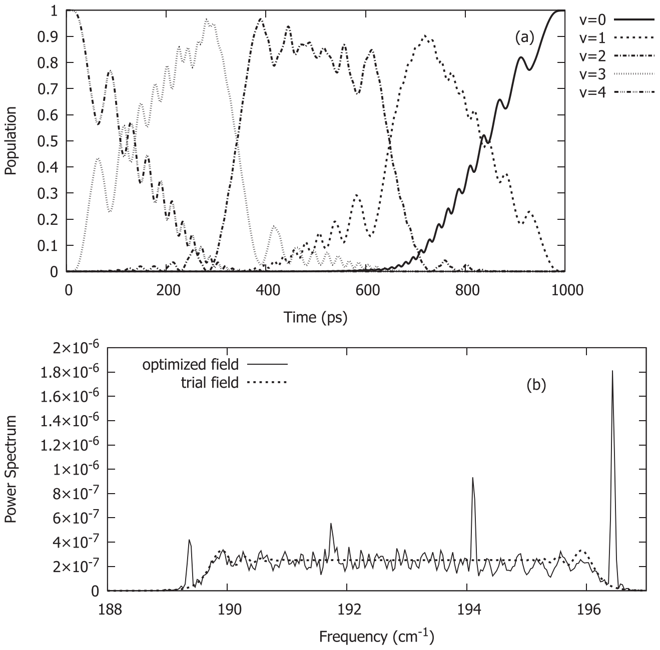

FIG. 6. (a) Population dynamics of the IR vibrational stabilization process with the optimized chirped pulse. (b) Power spectrum of the optimized pulse and of the linear chirped pulse.

Any $\alpha(t)$ which satisfies the above three coupled equations is a local optimal solution to the control problem. To numerically solve the optimal control problem, we apply the two-point boundary-value quantum control paradigm (TBQCP) scheme [76], in which $\alpha(t)$ is updated in the nth iteration according to

$$\alpha^{n+1}(t) = \alpha^n(t) - \eta_0 f_\mu^n(t), \tag{15}$$

where η_0 is a constant to be numerically adjusted for convergence and f_μ is the gradient $\delta J/\delta\alpha$,

$$f_\mu^n(t) = -2\mathrm{Im}\{\langle\chi^n(t)|\hat{\mu}|\psi^n(t)\rangle\}S(t)A\cos[\alpha^n(t)]. \tag{16}$$

The algorithm is started by choosing a trial control $\alpha^0(t)$ and solving the equation for the Lagrange multiplier (13). Then, the gradient is computed as the wave function is propagated forward in time.

Figure 6(a) shows the resulting population dynamics with the optimized chirped pulse built to perform the vibrational stabilization from the $\nu = 4$ to the ground level $\nu = 0$. To perform the optimization, we fixed the pulse envelope parameters and used as a trial pulse a linear chirped pulse, with the same chirping rate of Fig. 5(b). However, we used a comparatively smaller field amplitude of $A_{\rm ir} = 75$ kVcm^{-1}. The trial pulse yields only a population of the order of 10^{-3} in the ground level. After the optimization, the target-state population induced by the optimized pulse is roughly 0.999. Figure 6(b) compares the power spectrum of the trial linear chirped pulse with the power spectrum of the optimized pulse. The optimized pulse has a frequency modulation pattern around the plateau of the linear chirped pulse. It is also noticeable that the four main peaks observed in the spectrum correspond to the $\Delta\nu = -1$ transition frequencies between neighboring levels from $\nu = 4$ to the $\nu = 0$ ground level.

VI. CONCLUSION

In this work, we propose the combination of a pair of pump-dump pulses with a chirped IR pulse to perform the photoassociation of cold atoms along with the vibrational stabilization of the associated cold polar molecule. The proposed three-pulses scheme takes advantage of the high coupling of the initial collision state to an excited electronic states as compared to the electronic ground state. By performing part of the vibrational stabilization in the selected excited electronic state, it can avoid the *missing rung* problems implied in the ground-state-only stabilization. However, the scheme populates only a single electronic excited state, avoiding the complications of two pairs of pump-dump schemes, which usually involves two excited states. We also perform the optimization of the chirped IR pulse in a time domain, obtaining high yields in the ground vibrational level. Our calculations show that the optimized chirped pulses differs from a linear chirped pulse by a small modulation of the time-dependent frequency and by additional resonant frequencies. Therefore, our proposed methodology can be an alternative pathway to perform both photoassociation and vibrational stabilization aiming at forming cold or ultracold polar molecules. An optional scheme can also be conceived by replacing the pair of pump-dump pulses by a pair of STIRAP pulses starting from the continuum [29]. Finally, the vibrational stabilization with optimized chirped IR pulse could also be applied in conjunction with a magnetoassociation process to produce molecules in the vibrational ground level of the lowest triplet electronic state, as was recently proposed [53].

ACKNOWLEDGMENTS

E.F.L. acknowledges support from São Paulo Research Foundation, FAPESP (Grants No. 2023/04930-4 and No. 2014/23648-9) and from National Council for Scientific and Technological Development - CNPq.

---

[1] A. Yang, S. Botsi, S. Kumar, S. B. Pal, M. M. Lam, I. Čepaitė, A. Laugharn, and K. Dieckmann, Singlet pathway to the ground state of ultracold polar molecules, Phys. Rev. Lett. **124**, 133203 (2020).

[2] D. K. Ruttley, A. Guttridge, S. Spence, R. C. Bird, C. R. Le Sueur, J. M. Hutson, and S. L. Cornish, Formation of ultracold molecules by merging optical tweezers, Phys. Rev. Lett. **130**, 223401 (2023).

[3] T. P. Softley, Cold and ultracold molecules in the twenties, Proc. R. Soc. A **479**, 20220806 (2023).

[4] D. Mitra, K. H. Leung, and T. Zelevinsky, Quantum control of molecules for fundamental physics, Phys. Rev. A **105**, 040101 (2022).

[5] L. Levin, W. Skomorowski, L. Rybak, R. Kosloff, C. P. Koch, and Z. Amitay, Coherent control of bond making, Phys. Rev. Lett. **114**, 233003 (2015).

[6] E. F. de Lima, T.-S. Ho, and H. Rabitz, Laser-pulse photoassociation in a thermal gas of atoms, Phys. Rev. A **78**, 063417 (2008).

[7] J. Deiglmayr, M. Repp, O. Dulieu, R. Wester, and M. Weidemüller, Population redistribution in optically trapped polar molecules, Eur. Phys. J. D **65**, 99 (2011).

[8] R. Côté and A. Dalgarno, Mechanism for the production of $^6Li_2$ and $^7Li_2$ ultracold molecules, J. Mol. Spectrosc. **195**, 236 (1999).

[9] J. N. Byrd, J. A. Montgomery Jr., and R. Côté, Controllable binding of polar molecules and metastability of one-dimensional gases with attractive dipole forces, Phys. Rev. Lett. **109**, 083003 (2012).

[10] J. L. Bohn and P. S. Julienne, Semianalytic theory of laser-assisted resonant cold collisions, Phys. Rev. A **60**, 414 (1999).

[11] Y. Liu and K.-K. Ni, Bimolecular chemistry in the ultracold regime, Annu. Rev. Phys. Chem. **73**, 73 (2022).

[12] L. D. Carr, D. DeMille, R. V. Krems, and J. Ye, Cold and ultracold molecules: Science, technology and applications, New J. Phys. **11**, 055049 (2009).

[13] J. L. Bohn, A. M. Rey, and J. Ye, Cold molecules: Progress in quantum engineering of chemistry and quantum matter, Science **357**, 1002 (2017).

[14] A. V. Avdeenkov, D. C. E. Bortolotti, and J. L. Bohn, Field-linked states of ultracold polar molecules, Phys. Rev. A **69**, 012710 (2004).

[15] X.-Y. Chen, A. Schindewolf, S. Eppelt, R. Bause, M. Duda, S. Biswas, T. Karman, T. Hilker, I. Bloch, and X.-Y. Luo, Field-linked resonances of polar molecules, Nature (London) **614**, 59 (2023).

[16] M. Guo, B. Zhu, B. Lu, X. Ye, F. Wang, R. Vexiau, N. Bouloufa-Maafa, G. Quéméner, O. Dulieu, and D. Wang, Creation of an ultracold gas of ground-state dipolar $^{23}Na^{87}Rb$ molecules, Phys. Rev. Lett. **116**, 205303 (2016).

[17] P. K. Molony, P. D. Gregory, Z. Ji, B. Lu, M. P. Köppinger, C. R. Le Sueur, C. L. Blackley, J. M. Hutson, and S. L. Cornish, Creation of ultracold $^{87}Rb^{133}Cs$ molecules in the rovibrational ground state, Phys. Rev. Lett. **113**, 255301 (2014).

[18] T. Takekoshi, L. Reichsöllner, A. Schindewolf, J. M. Hutson, C. R. Le Sueur, O. Dulieu, F. Ferlaino, R. Grimm, and H.-C. Nägerl, Ultracold dense samples of dipolar rbcs molecules in the rovibrational and hyperfine ground state, Phys. Rev. Lett. **113**, 205301 (2014).

[19] J. Deiglmayr, A. Grochola, M. Repp, K. Mörtlbauer, C. Glück, J. Lange, O. Dulieu, R. Wester, and M. Weidemüller, Formation of ultracold polar molecules in the rovibrational ground state, Phys. Rev. Lett. **101**, 133004 (2008).

[20] S. Ospelkaus, A. Pe'er, K.-K. Ni, J. J. Zirbel, B. Neyenhuis, S. Kotochigova, P. S. Julienne, J. Ye, and D. S. Jin, Efficient state transfer in an ultracold dense gas of heteronuclear molecules, Nat. Phys. **4**, 622 (2008).

[21] C. R. Menegatti, B. S. Marangoni, and L. G. Marcassa, A review on the formation of heteronuclear cold molecules, Laser Phys. **18**, 1305 (2008).

[22] J. M. Sage, S. Sainis, T. Bergeman, and D. DeMille, Optical production of ultracold polar molecules, Phys. Rev. Lett. **94**, 203001 (2005).

[23] A. J. Kerman, J. M. Sage, S. Sainis, T. Bergeman, and D. DeMille, Production of ultracold, polar $RbCs^*$ molecules via photoassociation, Phys. Rev. Lett. **92**, 033004 (2004).

[24] A. V. Avdeenkov and J. L. Bohn, Linking ultracold polar molecules, Phys. Rev. Lett. **90**, 043006 (2003).

[25] E. Kuznetsova, P. Pellegrini, R. Côté, M. D. Lukin, and S. F. Yelin, Formation of deeply bound molecules via chainwise adiabatic passage, Phys. Rev. A **78**, 021402(R) (2008).

[26] R. Pires, M. Repp, J. Ulmanis, E. D. Kuhnle, M. Weidemüller, T. G. Tiecke, C. H. Greene, B. P. Ruzic, J. L. Bohn, and E. Tiemann, Analyzing feshbach resonances: A ^{6}Li $-^{133}$ Cs case study, Phys. Rev. A **90**, 012710 (2014).

[27] K.-K. Ni, S. Ospelkaus, M. H. G. de Miranda, A. Pe'er, B. Neyenhuis, J. J. Zirbel, S. Kotochigova, P. S. Julienne, D. S. Jin, and J. Ye, A high phase-space-density gas of polar molecules, Science **322**, 231 (2008).

[28] C. Warner, N. Bigagli, A. Z. Lam, W. Yuan, S. Zhang, I. Stevenson, and S. Will, Efficient pathway to NaCs ground state molecules, New J. Phys. **25**, 053036 (2023).

[29] E. Kuznetsova, M. Gacesa, P. Pellegrini, S. F. Yelin, and R. Côté, Efficient formation of ground-state ultracold molecules via STIRAP from the continuum at a Feshbach resonance, New J. Phys. **11**, 055028 (2009).

[30] J. Deiglmayr, P. Pellegrini, A. Grochola, M. Repp, R. Côté, O. Dulieu, R. Wester, and M. Weidemüller, Influence of a Feshbach resonance on the photoassociation of LiCs, New J. Phys. **11**, 055034 (2009).

[31] C. P. Koch and M. Shapiro, Coherent control of ultracold photoassociation, Chem. Rev. **112**, 4928 (2012).

[32] J. L. Bohn and P. S. Julienne, Semianalytic treatment of two-color photoassociation spectroscopy and control of cold atoms, Phys. Rev. A **54**, R4637(R) (1996).

[33] T. Franzen, B. Pollklesener, C. Sillus, and A. Görlitz, Intercombination-line photoassociation spectroscopy of ^{87}Rb^{170}Yb, Phys. Rev. A **107**, 023114 (2023).

[34] C. D. Bruzewicz, M. Gustavsson, T. Shimasaki, and D. DeMille, Continuous formation of vibronic ground state RbCs molecules via photoassociation, New J. Phys. **16**, 023018 (2014).

[35] E. F. de Lima, Coherent control of the formation of cold heteronuclear molecules by photoassociation, Phys. Rev. A **95**, 013411 (2017).

[36] K. Aikawa, D. Akamatsu, M. Hayashi, K. Oasa, J. Kobayashi, P. Naidon, T. Kishimoto, M. Ueda, and S. Inouye, Coherent transfer of photoassociated molecules into the rovibrational ground state, Phys. Rev. Lett. **105**, 203001 (2010).

[37] J. Ulmanis, J. Deiglmayr, M. Repp, R. Wester, and M. Weidemüller, Ultracold molecules formed by photoassociation: Heteronuclear dimers, inelastic collisions, and interactions with ultrashort laser pulses, Chem. Rev. **112**, 4890 (2012).

[38] K. M. Jones, E. Tiesinga, P. D. Lett, and P. S. Julienne, Ultracold photoassociation spectroscopy: Long-range molecules and atomic scattering, Rev. Mod. Phys. **78**, 483 (2006).

[39] M. Gacesa, S. Ghosal, J. N. Byrd, and R. Côté, Feshbach-optimized photoassociation of ultracold ^{6}Li^{87}Rb molecules with short pulses, Phys. Rev. A **88**, 063418 (2013).

[40] D. M. Reich and C. P. Koch, Cooling molecular vibrations with shaped laser pulses: optimal control theory exploiting the timescale separation between coherent excitation and spontaneous emission, New J. Phys. **15**, 125028 (2013).

[41] C. P. Koch, J. P. Palao, R. Kosloff, and F. Masnou-Seeuws, Stabilization of ultracold molecules using optimal control theory, Phys. Rev. A **70**, 013402 (2004).

[42] M. Ndong and C. P. Koch, Vibrational stabilization of ultracold krb molecules: A comparative study, Phys. Rev. A **82**, 043437 (2010).

[43] B. K. Lyu, J. L. Li, M. Wang, G. R. Wang, and S. L. Cong, Efficient formation of stable ultracold Cs_2 molecules in the ground electronic state via two-color photoassociation, Eur. Phys. J. D **73**, 20 (2019).

[44] A. Devolder, E. Luc-Koenig, O. Atabek, M. Desouter-Lecomte, and O. Dulieu, Proposal for the formation of ultracold deeply bound RbSr dipolar molecules by all-optical methods, Phys. Rev. A **98**, 053411 (2018).

[45] A. Devolder, M. Desouter-Lecomte, O. Atabek, E. Luc-Koenig, and O. Dulieu, Laser control of ultracold molecule formation: The case of RbSr, Phys. Rev. A **103**, 033301 (2021).

[46] E. F. de Lima, Optimal control of cold ground-state collisions by shaped laser pulses, J. Low Temp. Phys. **180**, 161 (2015).

[47] S. Kotochigova, Prospects for making polar molecules with microwave fields, Phys. Rev. Lett. **99**, 073003 (2007).

[48] Y.-Y. Niu, S.-M. Wang, and S.-L. Cong, Vibrational state-selectivity of product HI in photoassociation reaction $\mathrm{I} + \mathrm{H} \rightarrow \mathrm{HI}$, Chem. Phys. Lett. **428**, 7 (2006).

[49] E. F. de Lima and J. E. Hornos, Multiphoton association by two infrared laser pulses, Chem. Phys. Lett. **433**, 48 (2006).

[50] M. Korolkov, J. Manz, G. Paramonov, and B. Schmidt, Vibrationally state-selective photoassociation by infrared sub-picosecond laserr pulses: model simulations for $\mathrm{O} + \mathrm{H} \rightarrow \mathrm{OH}(\nu)$, Chem. Phys. Lett. **260**, 604 (1996).

[51] I. C. de Almeida and E. F. de Lima, Formation and vibrational stabilization of cold heteronuclear molecules by a single infrared pulse with time-dependent frequency, Laser Phys. **29**, 035501 (2019).

[52] T. Horiba, S. Shirai, and H. Hirai, Missing-rung problem in vibrational ladder climbing, Phys. Rev. A **105**, 013117 (2022).

[53] M. Londoño and J. C. Arce, Vibrational ladder-descending photostabilization of a weakly bound molecule: Quantum optimal control with a genetic algorithm, Phys. Rev. A **108**, 013301 (2023).

[54] C. Brif, R. Chakrabarti, and H. Rabitz, Control of quantum phenomena: Past, present and future, New J. Phys. **12**, 075008 (2010).

[55] A. Homer and G. Roberts, Chirped fields for $\mathrm{Rb} + \mathrm{Cs}$ photoassociation, Phys. Rev. A **78**, 053404 (2008).

[56] S. Kallush and Y. B. Band, Short-pulse chirped adiabatic population transfer in diatomic molecules, Phys. Rev. A **61**, 041401(R) (2000).

[57] E. Luc-Koenig, M. Vatasescu, and F. Masnou-Seeuws, Optimizing the photoassociation of cold atoms by use of chirped laser pulses, Eur. Phys. J. D **31**, 239 (2004).

[58] C. P. Koch, E. Luc-Koenig, and F. Masnou-Seeuws, Making ultracold molecules in a two-color pump-dump photoassociation scheme using chirped pulses, Phys. Rev. A **73**, 033408 (2006).

[59] J. L. Carini, S. Kallush, R. Kosloff, and P. L. Gould, Efficient formation of ultracold molecules with chirped nanosecond pulses, J. Phys. Chem. A **120**, 3032 (2016).

[60] J. L. Carini, S. Kallush, R. Kosloff, and P. L. Gould, Enhancement of ultracold molecule formation using shaped nanosecond frequency chirps, Phys. Rev. Lett. **115**, 173003 (2015).

[61] B. Kaufman, T. Paltoo, T. Grogan, T. Pena, J. P. S. John, and M. J. Wright, Pulsed, controlled, frequency-chirped laser light

at Ghz detunings for atomic physics experiments, Appl. Phys. B **123**, 58 (2017).

[62] P. J. Delfyett, D. Mandridis, M. U. Piracha, D. Nguyen, K. Kim, and S. Lee, Chirped pulse laser sources and applications, Prog. Quantum Electron. **36**, 475 (2012).

[63] M. C. Hoffmann and J. A. Fülöp, Intense ultrashort terahertz pulses: generation and applications, J. Phys. D **44**, 083001 (2011).

[64] R. Zhang, J.-W. Hu, G.-R. Wang, B. Fu, and Y.-C. Han, Steering photoassociation of cold ^{8}5Rb atoms by two-color slowly-turned-on and rapidly-turned-off laser pulses, J. Phys. B: At. Mol. Opt. Phys. **56**, 195201 (2023).

[65] W. Zhang, Y. Huang, T. Xie, G.-R. Wang, and S.-L. Cong, Efficient photoassociation with a slowly-turned-on and rapidly-turned-off laser field, Phys. Rev. A **82**, 063411 (2010).

[66] E. F. de Lima, T.-S. Ho, and H. Rabitz, Solution of the schrödinger equation for the morse potential with an infinite barrier at long range, J. Phys. A: Math. Theor. **41**, 335303 (2008).

[67] D. A. Fedorov, A. Derevianko, and S. A. Varganov, Accurate potential energy, dipole moment curves, and lifetimes of vibrational states of heteronuclear alkali dimers, J. Chem. Phys. **140**, 184315 (2014).

[68] N. Mabrouk, H. Berriche, H. B. Ouada, and F. X. Gadea, Theoretical study of the LiCs molecule: Adiabatic and diabatic potential energy and dipole moment, J. Phys. Chem. A **114**, 6657 (2010).

[69] A. Grochola, A. Pashov, J. Deiglmayr, M. Repp, E. Tiemann, R. Wester, and M. Weidemüller, Photoassociation spectroscopy of the $B\Pi_1$ state of $LiCs$, J. Chem. Phys. **131**, 054304 (2009).

[70] P. Staanum, A. Pashov, H. Knöckel, and E. Tiemann, $X\,^1\Sigma^+$ and $a\,^3\Sigma^+$ states of LiCs studied by Fourier-transform spectroscopy, Phys. Rev. A **75**, 042513 (2007).

[71] M. Aymar and O. Dulieu, Calculation of accurate permanent dipole moments of the lowest $^{1,3}\sum^+$ states of heteronuclear alkali dimers using extended basis sets, J. Chem. Phys. **122**, 204302 (2005).

[72] A. Derevianko, E. Luc-Koenig, and F. Masnou-Seeuws, Applications of *b*-splines in determining the eigenspectrum of diatomic molecules, Can. J. Phys. **87**, 67 (2009).

[73] H. Bachau, E. Cormier, P. Decleva, J. E. Hansen, and F. Martín, Applications of *b*-splines in atomic and molecular physics, Rep. Prog. Phys. **64**, 1815 (2001).

[74] J. Vala, O. Dulieu, F. Masnou-Seeuws, P. Pillet, and R. Kosloff, Coherent control of cold-molecule formation through photoassociation using a chirped-pulsed-laser field, Phys. Rev. A **63**, 013412 (2000).

[75] E. F. de Lima, T.-S. Ho, and H. Rabitz, Optimal laser control of molecular photoassociation along with vibrational stabilization, Chem. Phys. Lett. **501**, 267 (2011).

[76] T.-S. Ho and H. Rabitz, Accelerated monotonic convergence of optimal control over quantum dynamics, Phys. Rev. E **82**, 026703 (2010).